CHAPTER 2
Literature Review

2.1 Amorphous Silicon

Silicon is not found free in nature but appear chiefly as oxide and silicates. The structure of silicon can be classified into three categories, i.e crystal, amorphous and polycrystalline [1]. The polycrystalline silicon (98%pure) can be produced from metallurgical-grade silicon (MGS) through chemical reaction in the chemical vapour deposition process where the MGS is prepared commercially by heating silica and carbon in a submerged-electrode Arc furnace [2] using submerged graphite electrodes. Through the Czochralski technique [3], the single crystal silicon is then produced from the polycrystalline silicon and floating zone process does purification. For ultra-thin crystal silicon films preparation, advance epitaxy techniques [4] such as liquid phase epitaxy (LPE), vapour phase epitaxy (VPE) and molecule beam epitaxy (MBE) is used. Amorphous silicon (a-Si) can be prepared from the poly-silicon by thermal evaporate deposition technique or rf plasma sputtering technique. However, a-Si also can be prepare from silane using the plasma glow discharge deposition and a-Si produced by this technique is called as hydrogenated amorphous silicon [5] due to the presence of hydrogen in the material.

Crystal is defined by *Barret* (1952) as a structure consists of atoms arranged in a pattern that periodically in 3 dimension [6]. In crystal silicon, all atoms are arranged in order and complete bonded to all neighbors without any dangling bond. Therefore, crystal silicon is in a perfect order, where it has both the short-range order and long range order. Compared to crystal silicon, the structure of amorphous silicon is noncrystalline where it lacks long range periodical ordering and the atoms are randomly arranged in the lattice

networks. The orders in amorphous silicon are restricted only to few shell of neighbors, surrounding the central atom. As one goes further and further atoms, their distribution relative to the central atom become entirely random. So, the amorphous silicon has only short-range order. The actual structure of amorphous silicon consists of many voids with bonds, which are not joined by any atoms. These voids lead to interior dangling bonds, which can dominate the optical and electrical properties of amorphous silicon [7]. Therefore, amorphous silicon from different preparation technique has different structural formation which causes the difference in their properties. In hydrogenated amorphous silicon, the dangling bonds are sometimes filled by hydrogen atoms which improve the optical properties and this phenomenon attracted scientist to investigate on it. The most successful application of amorphous silicon is solar sell and thin film transistor (TFT) [8].

A distinction should be made between amorphous and polycrystalline silicon. Polycrystalline silicon is composed of grains with each grain containing a periodic array of atoms surrounded by a layer of interconnective or boundary atoms. Eventually for small enough grains such as microcrystalline, the distinction between the interior and surface is lost, and the concept of microcrystalline with a definable periodic region lose its meaning. While attempts have been made to model amorphous silicon by microcrystallite, it is now generally accepted that network models are more applicable.

2.2 Preparation Technique

Amorphous silicones which can not be prepared directly from the melt are usually fabricated in the form of thin films by an atomic deposition procedure such as sputtering, evaporation, chemical vapour deposition, plasma decomposition of gases or electroplating. Sometimes ion bombardment of crystal is used to leave an amorphous layer in the collision trail of the ion such as electron beam sputtering. Preparation technique is

very important since samples prepared from different technique are totally different in their structural and optical properties. This may be due to the fact that material source phase and energy transitions are different. Other conditions such as temperature, pressure, dilution gases and substrate material also influence the properties of amorphous silicon. This attracts scientist to develop new preparation technique and study their properties.

2.2.1 Thermal Evaporation

This method is most widely used for amorphous semiconductor preparation. The evaporation process is based on heating a material in a vacuum to a certain temperature thus causing a large number of atoms to acquire enough kinetic energy to leave the surface of the material and is then deposited on a substrate. The source energy usually is thermal from electric filament or electron beam bombardment [9]. Since the temperature required for every sample is different, the type of heating filament should be carefully selected. Because of low base pressure in the vacuum, most of the evaporated molecules experience no collisions with residual gas molecules and travel in straight lines to the substrate. However, the contaminating effect of residual gases must be considered. In some evaporation process, a stable gas such as Argon is employed to minimize this problem.

Figure 2.1 shows the schematic diagram of thermal evaporation where the entire system is built within a vacuum chamber with pressure of about 10^{-6} torr or lowers. The source material is placed on a high melting point metallic boat (usually molybdenum or tungsten) and current is passed through it to provide heat energy. As the material is heated to vaporization, it undergoes rapid transition from solid to the gaseous state and is deposited on the cold substrate in the form of thin amorphous films [10].

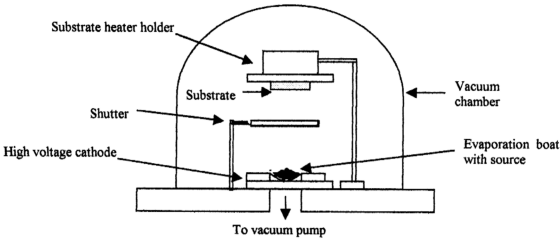

Figure 2.1 : A schematic illustration of an thermal evaporation system.

The disadvantage of this method is the films may not be good if there is contamination by impurities due to poor vacuum. The structure of amorphous silicon prepared from this technique is inhomogeneous.

Electron beam evaporation [11] is another advance evaporation technique, which is similar to thermal evaporation system except the metallic boat is replaced with copper boat and requires an electron gun system. Electrons are accelerated by the electron gun to high energy in beam and target to the material on copper boat. Energy transits to material atoms during bombardment of electron and causes these atoms to evaporate. The advantage of this technique is that the process can be done at room temperature and the temperature can be controlled using inductance heating.

2.2.2 Sputtering

Sputtering is the process whereby material in a solid target is ablated by bombardment with energetic ions from an electrical, low-pressure plasma struck in a gas. Ejected materials from the target, in the form of ionized atoms subsequently passes to a substrate where a film of target material is deposited. Usually, physical sputtering is used

with a non-chemically inert plasma gas (such as Ar). The target material is simply physically transported to the substrate and resultant film should have the same chemical composition as the target, since most elements have similar sputtering rates. However, some of the sputtering gas may be physically entrained in voids in sputtered film. If a reactive gas, e.g. O_2 or H_2 is used; a compound of the target material and the gas can be synthesized as a film. The simplest way to introduce sputtering is applying a high negative d.c voltage to the target, thereby attracting positive ions to etch the target surface. However, d.c sputtering is only feasible for target that are metallic or conducting materials where the target can act as electrode. This method wills therefore not work for insulating target materials, since the continuous bombardment of positive ions will charge the target to positive. In order to sputter poorly conducting materials such as silicon, an a.c field is capacitively coupled to the plasma at radio frequency (r.f) rate (13.6MHz) [12].

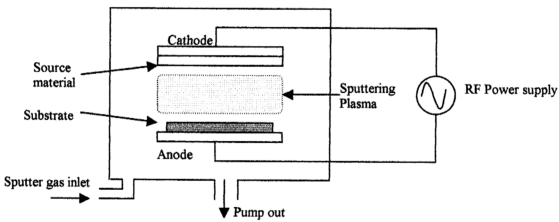

Figure 2.2 : Schematic diagram of a sputtering system.

Scientist at Harvard University makes the first sputtering hydrogenated amorphous silicon in 1974. Figure 2.2 shows the schematic diagram of radio frequency sputtering system [13] which consists of a reaction chamber, one target electrode, one

substrate electrode, pump system, a power and gas supply system. A base pressure of $< 10^{-4}$ Pa is maintained by an oil diffusion pump, and the sputtering gas is introduced in to the chamber at pressure of 0.1 to 1 Pa. Argon gas is normal used due to its non-reactive properties and its atomic weight. The polycrystalline silicon is bonded to cathode and the substrate to anode in the parallel-plate configuration. After striking the plasma by the RF power supply, the positive ions in the plasma are attracted towards the target during each negative half-cycle. However, the mobility of electrons in plasma is greater than ions, so more electrons than ions are attracted to the top surface of the target during the respective half-cycle, resulting in the build-up of a d.c negative bias of a few kV on the target. In steady-state conditions, therefore, the ions are attracted from the plasma to the target by this d.c bias. Sputtered ions from the target are carried towards the substrate by the following half-cycle of the r.f. field and deposited as a thin film of amorphous silicon.

Deposition rate for physical r.f sputtering are rather low, a few As^{-1}. The deposition rate can be increased significantly by the technique of magnetron sputtering, where a tailored, constant magnetic field around the target electrode concentrates the plasma density in the vicinity of the target surface, thereby increasing the flux of ablating ions from the plasma onto target. Futher details of the sputtering technique can be found in *Behrish* (1981,1983,1991)[14,15].

2.2.3 Chemical Vapour Deposition

Chemical vapour deposition (CVD) is the process where by reactive precursor vapour phase molecular species react, either homogeneously in the gas phase or heterogeneously at the solid-gas interface at the substrate surface, producing a film with a composition different from that of the starting materials. The precursor molecules can be made to decompose by means of heat (pyrolysis), absorption of UV light (photolysis) or in

electrical plasma formed in the gas [16]. Thermal CVD is the most commonly used method, which has the advantage that refractory material can be vapour-deposited at relatively low temperatures. Figure 2.3 show the conventional chemical vapour deposition apparatus of the silane pyrolysis.

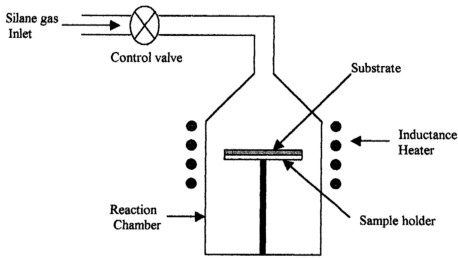

Figure 2.3 : Schematic illustration of an chemical vapour deposition apparatus.

Amorphous silicon film can be prepared from silane by using thermal CVD technique where the silicon substrate is heated to 200- 400C° for thermal decomposition of silane. This amorphous film may have impurities of hydrogen because of incompletely pyrolysis due to the lower temperatures. Reaction of pyrolysis is shown as below.

$$SiH_4(g) \xrightarrow[\Delta]{\text{Heat}} Si(s) + 2H_2(g)$$

As the substrate is heated to 600C° or higher, polycrystalline silicon can be produced from the complete pyrolysis of silane [17]. This technique is wisely used to produce high purity thin films of polycrystalline silicon.

Other sources of energy can be used to initiate molecular decomposition in CVD. One obvious alternative source is light where photons (typically in the UV region) with energy sufficient to break intra-molecular chemical bonds can cause direct dissociation, or facilitate dissociation in association with gas-phase collisions. An example of the application of this photo-CVD technique is the pyrolysis of disilane (Si_2H_6), thereby forming high quality films of hydrogenated amorphous silicon, a-Si:H, typically containing a few of % of chemically bonded hydrogen [18].

Another energy source that can be used to promote CVD is that associated with an electrical plasma; is termed as plasma-enhanced chemical vapour deposition (PECVD) or equivalently plasma glow discharge decomposition. It is normally used to produce thin film of amorphous or polycrystalline silicon, depending on the condition, from silane as precursor. The plasma decomposed by an electric field in a mixture of the feedstock gas (SiH_4) and a buffer gas (e.g. H_2, He or Ar), produces a thin amorphous silicon film on the substrate. The temperature of this technique can be lower (~200C°) than conventional thermal CVD, where higher temperature will cause chemical reaction of these gases. Electrical dopant such as P or B, can be incorporated substitutionally into films by admitting the gas phosphine (PH_3) or diborane (B_2H_6) into the feedstock gas flow.

2.2.4 Plasma Glow Discharge Decomposition

Plasma glow discharge decomposition technique also known as plasma enhance CVD, which is widely used to produce amorphous silicon thin film from the gas silane (SiH_4) and become very important in the thin film device application such as amorphous solar cell, printing head and TFT transistor [8]. The quality and properties of amorphous silicon prepared from this technique is greatly influenced by the growth conditions such as parameters of gas pressure, concentration of silane, flow-rate, radio frequency power, type

of gas dilution, substrate materials and temperatures [19]. The majority of glow discharge produces mostly neutral fragment of silane.

Plasma glow discharge deposition of amorphous silicon was first carried out in an inductively coupled system by *Sterling* and his collaborators [20] at the Standard Telecommunication Laboratories in Harlow, England. The glow discharge system is a vacuum reaction chamber consist of two electrodes for discharge, a mixing chamber, a vacuum pump, a direct current or radio frequency power supply and gas supply for instants silane and other dilution gases. Figure 2.4 shows the schematic diagram of plasma glow discharge decomposition system.

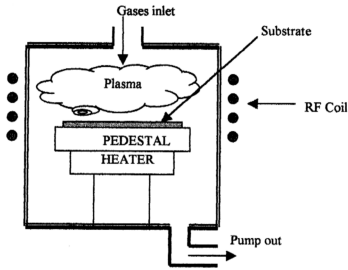

Figure 2.4 : Schematic illustration of an conventional plasma glow discharge decomposition apparatus.

In this technique, the silicon is deposited on a heated substrate (some process requires room temperature depend on the situation) as a result of a gaseous hydride of silane. Sometime, dilution with other gases is required to improve the quality of amorphous silicon such as H_2. These gases are flow into a fused silica reaction tube

through a gas flow-meter which control their flow-rates. The pressure lies in the range from o.1 to1 torr at standard temperature. A rotary pump, sometimes fitted with a root blower, is required to maintain gas flow and the pressure at precise value. The substrate is held on the heated pedestal, which is immersed, in the lower part of the glow discharge plasma. The plasma struck in a mixture of silane gas and dilution gas after the electric field (usually is radio frequency and typically 13.6MHz) is applied. This causes the precursor molecules to dissociate into ions and neutral free radicals (e.g. SiH_3•) in the gas phase by means of electron collisions. These species then impinge on a moderately heated substrate (~200C°) to form an amorphous film. If the glow discharge is diluted with other gases, the temperature should not be too high since silane will react with the dilution gas (e.g. Argon will react with silane at temperature over 500C°). For the substrate heated above 700C°, polycrystalline silicon is produced. Finally, a detoxification system is necessary to remove the non-reacted gases in the system such as silane which very dangerous.

2.2.5 D.C Plasma Glow Discharge Decomposition with Argon Dilution.

The d.c plasma glow discharge decomposition of silane with argon dilution is the technique using to prepare the hydrogenated amorphous silicon (a-Si:H) film studied in this work. This technique is a modification from the conventional plasma glow discharge decomposition. In this technique, d.c power supply is using to create the plasma glow discharge of silane. Argon is a metastable atom and non-chemical reactive gas, whish is mixing with the silane in the deposition chamber to dilute the discharge of the silane. The substrate is hold on the anode electrode and a-Si:H is deposited as thin film on the substrate surface due to electric field . The other condition is almost the same with the plasma glow discharge technique.

Argon always used as passive diluent gas is believed play an important role in the growth mechanism of the deposited materials. During the process of discharge, argon is excited by the electron energy in the plasma and transfers the energy to the silane for discharge. Thus, argon dilution can enhance the association of the silane and therefore enhance the deposition rates of the materials [21]. Argon dilution is strongly affected the materials properties of the film depending on the preparation parameters. The discharge of argon in the plasma also causes the bombardment of argon ion on the growth zone of he materials that can have the beneficial and detrimental effects on the materials properties depending in the preparation condition [22]. These effects had attracted the attention of researchers to further studies on it.

2.3 Structure of Amorphous silicon

Amorphous silicon is a solid in which the atomic size is randomly arranged and is completely covalent semiconductor. Structure of amorphous silicon consists of 4 silicon atoms that are bonded in tetrahedral form as illustrated in figure 2.5. The atoms in tetrahedral form are randomly orientated with respect to each other. The early knowledge of amorphous silicon came from x-ray and electron diffraction experiment, in which the radial density function obtained [23,24] shows that atoms are bonded in a tetrahedral form with an average corresponding to crystalline silicon structure. Base on these results [25], several models for the structure of amorphous silicon have been proposed. A simple possibility is that the amorphous silicon is made up of microcrystallite silicon about 20Å in extent [26]. Another model is based on the diamond and wurtzite lattice whish have identical tetrahedrally coordinated nearest-neighbour environment. The second nearest neighbour environment of these structures are differ by 180° rotation in the conjugation of the tetrahedral bonding structure as figure 2.6 [27]. The diamond lattice having only

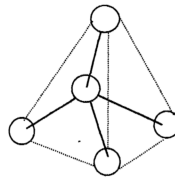

Figure 2.5 : The tetrahedral bond in amorphous semiconductor.

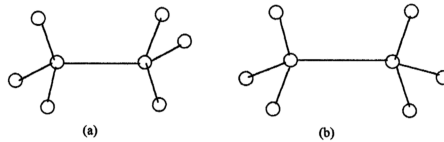

Figure 2.6: (a) Chain configuration or "staggered" configuration for tetrahedral bonded structure.
(b) Rotation of 180° is necessary to obtain "eclipsed" configuration for tetrahedral bonded structure.

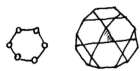

Figure 2.7(a) : structure of diamond lattice

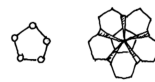

Figure 2.7(b): structure of ***amorphons***.

chain-like or 'staggered' six-membered rings and the Wurtzite structure having one-quarter boat-like or 'eclipsed' five-memebered rings.

Grigorovici and *Maniala* [28] point out that the five-memebered rings can build up to form isocahedral array in which twenty tetrahedron centers occupy the corners of a regular dodecahedron. They called such structure as "***amorphons***" and proposed that amorphous silicon is a mixture of half diamond unit and half amorphons. Structure of diamond lattice and "amorphons" is illustrated in figure 2.7. Independently, *Coleman* and *Thomas* [29] proposed a similar model but based on 60%diamond- 40% amorphons ratio. In 1971, *Polk* [30] constructed a random network model, in which all atoms are surrounded by 4 covalent bonded silicon at the proper interatomic separation and the deviation in bond is allowed. The random network concept is first proposed by *Zachariasen* [31] in 1932. Based on Polk model, the average angle of the tetrahedral structure is 109°28' with average deviation of ±10° and maximum at ±20°. Through extensive scanning electron diffraction studies, *Moss* and *Graczyk* [32] found that the random network model of *Polk* fitted to their diffraction data very well where a bond angle distortion of as much as 20° were found to be completely in accordance with the model of *Polk*.

Based on these structural results, the most ideal amorphous state [33,34] is with near perfect short-range but no long-range order. Such a state has no internal dangling bond and all valance requirements in the interior are locally satisfied. This state is metastable and represents a minimum local energy atomic arrangement. However, for most of deposited amorphous silicon, there are many voids within the structure. These voids lead to interior dangling bonds and mostly dominate the electrical and optical properties of amorphous silicon. These voids can be removed by annealing the amorphous silicon films below the crystallization temperature.

2.4 Optical Properties

Optical properties of amorphous semiconductor are generally influenced by the electronic and lattice properties [7]. Electronic properties concern processes involving the electronic states of a solid, while lattice properties involve the vibration of the lattice. These mechanisms cause the optical absorption in the solid. It involves coupling of the electric vector of the incident radiation to dipole moments in the material and consequent transfer of the energy. Analysis of the optical absorption of thin film, give the conclusion regarding the refractive index, optical band gap, dispersion energy, oscillator energy, Urbarh Tail bandwidth and etc.

2.4.1 Absorption Edge

Absorption happens when an electron receives energy from the incident photon and jumps from the valence band into the conduction band [7]. This electronic transition start at the absorption edge, which corresponds to the minimum energy difference E_g between the lowest valence band and the highest conduction band. So, the photon energy must be equal or larger than the energy gap, $h\nu \geq E_g$, where E_g is the energy gap and ν is the frequency of the photon. The frequency $\nu_o = E_g/h$ can be defined as the absorption edge.

When the semiconductor become amorphous, the absorption edge will shift either lower or higher energies. The absorption coefficient increase parabolically with the frequency above the absorption edge ($\nu > \nu_o$). Figure 2.8 is the schematic of the absorption spectrum of amorphous semiconductor. When the absorption of light passes through materials, it varies with wavelength. For this situation, absorption is expressed in terms of coefficient.

There are three regions in absorption spectrum. Region A represented a high absorption region ($\alpha > 10^4$ cm^{-1}). High value of α is cause by transitions from the

localized valence band states above E_g or the other way around. Region B almost same with those observation in the crystalline semiconductor. This exponential region has an absorption coefficient which lies in the range of $1 < \alpha < 10^4$ [6].

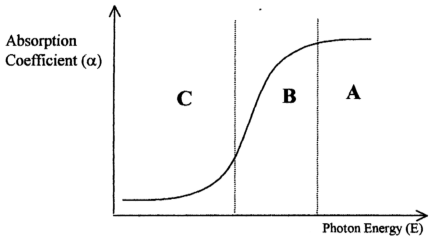

Figure 2.8: Schematic absorption spectrum graph for amorphous semiconductor.

The absorption region which varies exponential with photon energy, E is the region within region B, where the Urbach Tail bandwidth, E_e can be determined. E_e is the inversion of the slope determined from the graph of $\ln\alpha$ versus E which is in the range between 0.05 eV and 0.08 eV. The absorption coefficient in this region is due to the transitions between the tail states in one band and extended states in the other band.

The region C is the weak absorption tail. This optical properties may be caused by the initial and either the final states being localized at one or different centers. Transition at different center is due to electron transfer from an impurity ion to an ion of the most lattice or vice versa. The transitions can also happen between localized initial states and extended final states or vice versa.

2.4.2 Optical Properties of Thin Semiconducting Films

The most direct and simplest method of studying the band structure of a semiconductor is from its optical absorption spectrum. The absorption spectrum is unique for every material because, during absorption process, an electron will be excited only by photon with certain energy, to higher energy states within the semiconductor. By studying the transmission spectrum, one can investigate some of the possible quantum mechanical transitions of semiconductor electrons and learn much about the distribution of allowed electronic energy levels.

From the optical data, one can obtain considerable information on the electronic structure of the semiconductor film. The optical constants that can be obtained from the transmission data are refractive index, absorption coefficient, extinction coefficient and the thickness of the film. From these parameters, many others useful information could be obtained; such as optical density, energy gap, various characteristic energies, dielectric constant, density of valence electron and etc [35].

The optical transmission of thin film required the film to be deposited on a transparent substrate, which have no effect on the absorption spectrum within the wavelength region analyzed. The practical situation for a thin film on a transparent substrate is shown in figure 2.9, where the film has thickness d bounded by two media with refractive indices N_0 and N_2. The transmission $\boldsymbol{T}$ and reflection $\boldsymbol{R}$ of this system is given by [36]

$$\boldsymbol{T} = \frac{\boldsymbol{T_{23}T_{02}}}{\boldsymbol{1 - R_{20}R_{23}}} \tag{2.1}$$

and

$$\boldsymbol{R} = \frac{\boldsymbol{T_{20}^2 R_{23}}}{\boldsymbol{1 - R_{20}R_{23}}} + \boldsymbol{R_{02}} \tag{2.2}$$

where $T_{02} = T_{20} = \frac{n_2}{n_0}\left|\frac{e_1 t_{01} t_{12}}{1 - e_1^2 r_{10} r_{12}}\right|^2$, $R_{02} = \left|r_{01} + \frac{e_1^2 t_{01} t_{10} r_{12}}{1 - e_1^2 r_{10} r_{12}}\right|^2$

$R_{20} = \left|r_{20} + \frac{e_1^2 t_{21} t_{12} r_{10}}{1 - e_1^2 r_{12} r_{10}}\right|^2$, $T_{23} = \frac{n_3}{n_2}|t_{23}|^2$

$R_{23} = |r_{23}|^2$, . $e_1 = \exp\left(\frac{2i\pi N_1 d}{\lambda}\right)$

$t_{kl} = \frac{2N_k}{N_k + N_1}$, $r_{kl} = \frac{N_k - N_l}{N_k + N_l}$

$N_k = n_k + ik_k$

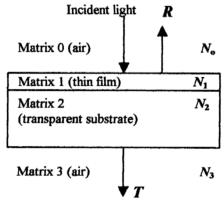

Figure 2.9: A type transmission ***T*** and reflectance ***R*** of light in thin film on a transparent substrate.

The exact expression of ***T*** in air-film-substrate-air interfaces where refractive indices $No = N_3 = 1$, $N_1 = n + ik$ and $N_2 = n_s$ is given [37] as

$$T = \frac{Ax}{B - Cx + Dx^2} \tag{2.3}$$

where $A = 16n_s\left(n^2 + k^2\right)$

$B = \left[(n+1)^2 + k^2\right]\left[(n+1)\left(n + n_s^2\right) + k^2\right]$

$$C = \left[\left(n^2 - 1 + k^2\right)\left(n^2 - n_s^2 + k^2\right) - 2k^2\left(n_s^2 + 1\right)\right]2\cos\left(\frac{4\pi nd}{\lambda}\right)$$
$$- k\left[2\left(n^2 - n_s^2 + k^2\right) + \left(n_s^2 + 1\right)\left(n^2 - 1 + k^2\right)\right]2\sin\left(\frac{4\pi nd}{\lambda}\right)$$

$$D = \left[(n-1)^2 + k^2\right]\left[(n-1)\left(n - n_s^2\right) + k^2\right)$$

and $$x = \exp\left(\frac{-4\pi kd}{\lambda}\right) = \exp(-\alpha d) \qquad (2.4)$$

α is the absorption coefficient of the thin film at wavelength λ. In medium with weak absorption region where $k^2 \cong 0$, equantion (2.3) reduces to equation (2.5)

$$T = \frac{16n_s n^2 x}{c_1 + c_2 x^2 - 2\left(n^2 - 1\right)\left(n^2 - n_s^2\right)x\cos\left(\frac{4\pi nd}{\lambda}\right)} \qquad (2.5)$$

where $c_1 = (n+1)^3(n + n_s^2)$ and $c_2 = (n-1)^3(n - n_s^2)$.

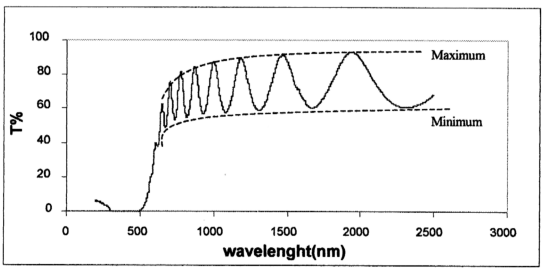

Figure 2.10: The typical transmission spectrum of amorphous thin film.

A typical transmission spectrum of a thin film is shown in Figure 2.10. The interference fringes observed are due to interference of the multiply reflected beams in the

film. The number of interference peaks is increased with increasing film thickness. The basic equation for the fringes at its maxima and minima is given by

$$2nd = m\lambda \tag{2.6}$$

and

$$2nd = (m + 0.5)\lambda \tag{2.7}$$

respectively, where integer m is the order of the interference fringes. The transmission maxima T_{max} and minima T_{min} is given by incorporating equation (2.6) and (2.7) into equation (2.5) such that

$$T_{max} = \frac{16n_s n^2 x}{c_1 + c_2 x^2 - 2(n^2 - 1)(n^2 - n_s^2)x} \tag{2.8}$$

$$T_{min} = \frac{16n_s n^2 x}{c_1 + c_2 x^2 + 2(n^2 - 1)(n^2 - n_s^2)x} \tag{2.9}$$

An expression which is independent of x could be yielded by substrating the reciprocal of equation (2.8) from the reciprocal of that equation (2.9), such that

$$\frac{1}{T_{min}} - \frac{1}{T_{max}} = \frac{(n^2 - 1)(n^2 - n_s^2)}{4n_s n^2} \tag{2.10}$$

solving equation (2.10) for n yields

$$n = [N + (N^2 - n_s^2)^{1/2}]^{1/2} \tag{2.11}$$

where

$$N = \frac{1 + n_s^2}{2} + 2n_s \frac{T_{max} - T_{min}}{T_{max} T_{min}}$$

Equation (2.11) can be used to calculate $n(\lambda)$ from T_{max} and T_{min}. It is identical to the formula derived by *Manifacier et al* [38] using the theory for an infinite substrate. Once $n(\lambda)$ is known, α can be determined from both equation (2.8) and (2.9) by solving the quadratic equation for x. Similar results can be obtained by adding the reciprocals of equatiion (2.8) and (2.9) such that

$$x = \frac{F - \left[F^2 - (n^2 - 1)^3 (n^2 - n_s^4)\right]^{-1/2}}{(n-1)^3 (n - n_s^2)} \tag{2.12}$$

where $$F = \frac{4n^2 n_s (T_{max} + T_{min})}{T_{max} T_{min}}$$

According to *Manifacier*, the thickness of the film can be determined from two maxima or minima using equation (2.6) and (2.7) such that

$$d = \frac{M\lambda_1\lambda_2}{2[n(\lambda_1)\lambda_2 - n(\lambda_2)\lambda_1]} \quad (2.13)$$

where M is the number of oscillations between the two extreme. λ_1, $n(\lambda_1)$, λ_2 and $n(\lambda_2)$ are the corresponding wavelengths and refractive indices. Knowing d and α, extinction coefficient k can be calcuulated from equation (2.4).

Thickness of the films can also be determined by using Tolansky technique[39] of equal frines shift and x-ray diffraction method [40]. The Tolansky technique basically utilizes the formation of interference fringes from a wadge shape film of air between parallel plates. If observation is made almost normal to the film, the condition for bright and dark fringes are in equations (2.6) and (27). The optical thickness of the film changes by $\lambda/2$ for the next fringes. If a thin layer of film is deposited on the lower plate, the fringes observed at the thin film-plate boundary will be shifted since the optical path is different. This shift could be used to calculated the thickness of the film through the equation below

$$d = \frac{\lambda}{2}\left(\frac{b}{a}\right) \quad (2.14)$$

where d, λ, a, b are film thickness, wavelength of light source, distance between the adjacent bright fringes and the fringe shift respectively.

Various techniques have been developed to determine these optical constants. *Davis et al* [41] used the basic equation from (2.6) and (2.7) to determine the refractive index of the film where, in this case, n is calculated by guessing the initial value of the integer m. An accurate guess of m will yeild a nearly constant refractive index at long

wavelength wich increase toward shorter wavelength. Otherwise, spurious results such as a decrease in n toward shorter wavelength is obtained. In this case, the technique is a combination of *Davis* and *Manifacier* technique where Manifacier techniqur is used to determine the n at the optomum (maximum or minimum) at the longest wavelength of the transmission spectrum. The wavelength posistion of the maximum and minimum in the spectrum is then located. Thereby using the equation $2nd=m\lambda$ where m=0, 0.5, 1, 1.5,……, the graph of nd versus $\lambda/2$ is plotted. A accurate value of m is chose as a curve decreasing with λ in a Cauchy expression (a+b/2) is appeared. The thickness, d at the longest λ is then determined by using the accurate m. The d is then used to determine the n at the maximum and minimum of the spectrum. Finally, the graph of n versus $1/\lambda$ is plotted and the parameter of a and b is determined. The refractive index for the whole spectrum can be determined by using the Cauchy relation where parameter a is the value of the refractive index, n. This refractive index, n of the spectrum is fitted to the saturated n as the wavelength increasing to infinute. Thus, n is always used as the true or applicable refractive index of the film.

On the other hand, *D. Bhattacharyya et al* [42] used the expression $T/(1-R)$ in determining n which can be beyond the absorption edge without any prior assumption of film parameters.

2.4.3 Refractive Index (n)

The refractive index, n of any optical medium is defined as the ratio of light speed in vacuum to light speed in the medium. In the thin film properties, the n is measured from the transmission and reflection of the incident light and is greatly related to the bulk density of a film. The lattice arangement of medium can affect the speed of light, thus can affect the refractive index. High bulk density have high value of refractive index

due to the microstructure properties. For the factor of surface morphology, the columnar structure on the surface of film also have the reduce the value of n because lower bulks density could be due to columnar structure [43,44]. In this work, the n is determined from the transmission spectrum using the *Manifacier* and *Davis* methods which is shown in chapter 3. The preparation condition is also important factor that affected the n because the optical properties and the structure properties is greatly depend on the preparation parameter.

2.4.4 Optical Energy Gap (E_g).

The optical energy is defined as small energy difference between the boundaries of the localized states in the valence and the delocalized states in the conduction band. According to *Tauc* [6], the optical energy gap is related to the absorption constant by the following equation.

$$\alpha E = A(E-E_g)^2 \tag{2.15}$$

where E is the photon energy, E_g is the optical energy gap, α is the absorpton coefficient and A is the constant.

From the plot $(\alpha h\nu)^{1/2}$ as a function of $h\nu$ in the strong absortion region as figure 2.11, the optical energy gap can be obtained using the expression,

$$(\alpha h\nu)^{1/2} = A^{1/2}h\nu - A^{1/2}E_g \tag{2.16}$$

By using the regression method, the slope of the plot $(\alpha h\nu)^{1/2}$ as a function of $h\nu$ and the intersection with the energy axis can be determined. Since the slope, $m = -A^{1/2}$ and the intersection is $c = A^{1/2}E_g$, thus :

$$E_g = -c/m \tag{2.17}$$

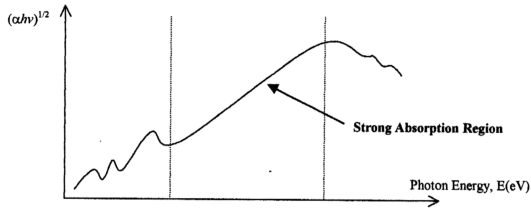

Figure 2.11 : Plot of $(\alpha h\nu)^{1/2}$ versus photon energy, E.

According to *Freeman* and *Paul* [45], the band gap in pure amorphous silicon is about 1.3eV and typically lies between 1.7 to 2.0 eV in hydrogenated amorphous silicon (a-Si:H) films. The variability of the results is due to ion bombardment and impurity incorporation. The preparation technique and condition also are the factor that affect the energy gap of the a-Si:H films. By using a low pressure hydrogen deficient (H_2/Ar) plasma in sputtering method, *Ross* and *Messier* [43] report that sputtered a-Si:H films with band gap as low as 0.55eV is attainable. Such films were stable and had a very amorphous microstructure, which is due to he beneficial effects of argon ion bombardment on the film growth surface.

Since a-Si:H consist of hydrogen that related to the microstructure, the optical energy gap also dependent on defects of the pure silane matrix and the actual hydrogen content of the film. Based on the studies on plasma glow discharge a-Si:H film [46], *Tanaka* explained that optical energy gap of glow discharge a-Si:H films is mainly determined by the amount of the bonded H and the effects of annealing decrease the optical energy gap of a-Si:H film depending on the temperature. At annealing temperature higher than 350°C, the optical energy gap decrease because the film release their hydrogen.

2.4.5 Urbach Tail Bandwidth (E_e).

The Urbach Tail bandwidth exists caused by the configuration disorder in the amorphous silicon. Based on *Anderson's theory* [47], *Mott* [48] argued that the spatial fluctuatiion in the potential caused by the configuration diorder in microstructure of amorphous silicon may lead to the formation of localized states, which do not occupy all the difference energies in the band, but form a tail above the valence band and below the conduction band. The localized donor state occurs above the conduction band, while the localized acceptor state occurs below the valence band.

The $\boldsymbol{E_e}$ can be deduced from the slope of plot $\ln(\alpha)$ versus photon energy where α is absorption coefficient. Since $\boldsymbol{E_e}$ is related to the width of the band tails in the absorption edge, the absorption coefficient is depended exponentially with the band energy as given below:

$$\alpha = \alpha_o \exp[\,(E-E_o)/\boldsymbol{E_e}\,] \qquad (2.18)$$

where, E is the photon energy, α_o and E_o are experimentally determined factors.

$$\ln(\alpha) = \ln(\alpha_o) + [\,(E-E_o)/\boldsymbol{E_e}\,] \qquad (2.19)$$

From the plot of $\ln(\alpha)$ versus E, the slope is $m = 1/\boldsymbol{E_e}$ and thus $Ee = 1/m$

2.5 Effects of Argon (Ar) Dilution.

Argon dilution has been known greatly affects the properties of plasma deposited a-Si:H films. Due to the metastable and non-chemical reactively behavior, argon (Ar) always used as inert gas to dilute the plasma deposited a-Si:H film in order to enhance the deposition rates and improve microstructural properties of a-Si:H film. From the reports of researchers, it has been known that involve of argon in the plasma will have argon ion bombardment and argon incorporation effects. From the researches of *Moustakas* [49], it is well known that argon atom is inevitablly incorporated into plasma

deposited a-Si:H as an impurity depending on deposition condition such as gas pressure and rf power. *Anudujar* [50] has been reported that the Ar^+ ion bombardment of a-Si:H during growth can be have both beneficial and detrimental effects on materials properties. These important information had encouraged future studies of argon dilution in plasma deposited a-Si:H materials.

In the studies of the role of argon involved in plasma deposited a-Si:H, *T.Tanaka* [46] suggested that argon atom plays the role of steric hindrance against H_2 diffusion and also thermal rearrangement of H. Argon is noted never evolved at least up to 400°C. From the annealing studies involved the characterization of EPMA experiment, nearly 8 atom % of Ar has been detected both in sputtering a-Si:H films by Electron Probe Micro Analysis (EPMA) while 1 atom % in glow discharge a-Si:H samples. The EPMA traces also shown that Ar atom incorporated in the films never effuse at least up to 400°C, but evolution of Ar occurs explosively at 450-500°C for some sample depending on film thickness. The Ar content increase with an increase in rf power is found through the EPMA spectra. Through the FTIR characterization experiment, the phenomenal tendency of the FTIR results is strongly correlated with Ar content of each film. Films involving a larger amount of Ar release their hydrogen at higher temperatures compared with Ar-poor film. Thus, it suggests that Ar in a-Si:H films play the role of steric hindrance against H diffusion and microscopically, Ar atom seems to inhabit a structural defect (possibly a void) associated with dihydride. From the experiment results, *T.Tanaka* [46] also concluded that the presence of Ar is strongly correlated with high ratio of dihydride to monohydride mode absorption which might be responsible for low quantum efficiencies of photoconductivity and photoluminescence in a-Si:H film.

In the studies of argon dilution effects on the structure of microcrystalline silicon, *U.K. Das* [51] has observed that argon not only as a passive diluent gas but also

plays an important role in the growth of the amorphous or microcrystalline network. In the film deposited with 95% argon dilution revealed in the TEM studies, the inhomogeneities on the scale of 50nm is observed in the micrograph that probably results from the variation of amorphous material. Increase of Ar dilution to 98% and keeping the rf power density results in the formation of microcrystallites. At 99% argon dilution and low rf density, the film is almost homogeneously amorphous. Data from the Raman scattering studies also indicated that the microcrystalline samples prepared from argon dilution appear to contain microcrystals of difference sizes. A very small but definite contribution in 510-520 cm^{-1} range indicated the presence of isolated small crystallites in amorphous sample.

From the results of the structure studies by FTIR, Raman spectroscopy and TEM, *U.K. Das* [51] found several important point that microcrystal grain start to develop within a denser region which may result from large scale structural variation in the bulk when argon is increased beyond 95%; There is a sharp increase of clustering of the microcrystallites when argon is increased from 98% to 99% at a moderate rf power density of 80 mW/cm^2; Raman spectra reveal the presence of well-separated small microcrystal distributed in the amorphous matrix even in case of predominantly amorphous type samples; The hydrogen content is high in the argon diluted amorphous and microcrystalline sample where hydrogen is predominantly bonded in monohydride mode.

U.K. Das [51] proposed a model based on energy exchange between the excited Ar* state and the growth zone of the materials to explain the structural changes in the presence of argon in the plasma. It is proposed that energy released from deexcitation of Ar^+ and Ar* which bombard the surface at thermal velocities is used in breaking up of strained weak Si-Si bonds at the boundary of the c-Si nucleation centers and the amorphous matrix. Hydrogen bonded in the amorphous matrix surrounding the nucleation

centers also diffuses out creating a compact hydrogen-free zone. Amorphous region outside this compact zone, however, contains a lot of bonded hydrogen. Development of large size microcrystallites thus requires formation of such heterogeneous structure containing localized hydrogen-depleted region.

On the other hand, *H. Meiling* [21] reported in the studies of high deposition rate a-Si:H from argon diluted silane that argon dilution effectively enhance the dissociation of silane, and therefore to enhance the deposition rate, through quenching of excited metastable argon atom, Ar* on silane molecules. The energy transfer during bombardment of argon ion, enhances the surface diffusive of precursor and eliminates clustered H from the film, resulting in the observed improvement of structure properties of a-Si:H film.

2.6 Surface Morphology Studies of Atomic Force Microscopy (AFM).

The atomic force microscope (AFM) was developed from the Scanning Tunneling Microscope (STM) in 1986 by *Binning, Quate* and *Gerber* [52]. Like all the other Scanning Probe Microscopes, the AFM utilizes a sharp probe moving over the surface of a sample in a raster scan. The probe is a tip on the end of a cantilever, which bends in response to the force between the tip and the sample. The first AFM used a scanning tunneling microscope at the end of the cantilever to detect the bending of the lever, but now most AFM employ an optical lever technique. Figure 2.12 is the diagram that illustrates how it works; as the cantilever flexes, the light from the laser is reflected on to the split photo-diode, by measuring the difference signal (A-B), changes in the bending of the cantilever can be measured. The details of the scanning operation will be presented in chapter 3 later. The image scanned from AFM is viewing in 3-dimension picture which more advantage compared to 2-dimension image from the SEM and TEM microscopy.

Some homogeneous surface of a-Si:H films that cannot detected in SEM and TEM, however can be shown clearly utilizing the AFM. Figure 2.13 below show the example image of a-Si:H film scanned utilizing the AFM.

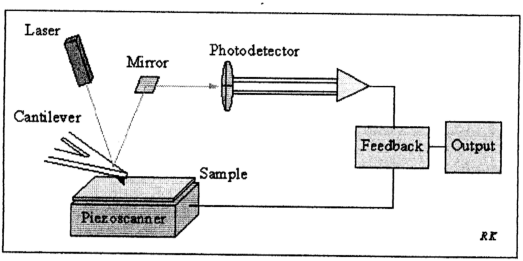

Figure 2.12: Diagram of AFM working system included the interaction of optical and detecting system.

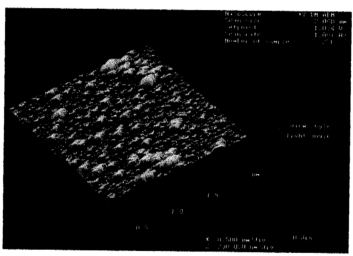

Figure 2.13 : Image of a-Si:H sample scanned by AFM.

From the early microstructure studies utilizing the SEM, *J.Knights* [53] reported that the plasma deposited a-Si:H films from silane or silane/argon mixtures proceeds via nucleation and growth of islands structure of average dimensions ~100Å. If these islands do not coalesce into a homogeneous film, subsequent growth produces columnar morphology with low-density interstitial regions. There is strong correlation between the columnar structure and the presence of non-radiative recombination centers. Knights also concluded that the microstructure of plasma deposited a-Si:H is strongly influenced by varying parameters of the deposition process.

Daewon Kwon [54] utilizes the AFM to investigate the microstructure at the surface of thick (>4000Å) a-SI:H films prepared from glow discharge as well as hot wire chemical vapour deposition (HWVCD) techniques. The imaging was performed by operating the AFM in "Tapping mode" with a "Nanoscope III" (Digital instrument, Inc.). All the a-Si:H film exhibit a distinct granular morphology while the somewhat different (Wavier) surface morphology is observed in the HWVCD prepared a-SI:H films. The average grain size in the microstructure of a-Si:H films varied between 40nm and 90nm as the substrate temperature was change and also as the different gas mixtures were employed during the growth. The grain size was reduced with increasing substrate temperature no matter what growth methods were employed. Gas dilution with argon and hydrogen also resulted in grain size reduction of a-Si:H film as observed in AFM images.

In the photoconductivity and density of states studies of a-Si:H film prepared from PEVCD technique, *Budaguan* [55] observed the a-Si:H films posses a relatively regular microstructure consisting of "grain" with characteristic size of 300-500Å utilizing the AFM. This regular microstructure is found in all fabricated samples while the concentration and the size of the "grain" depend on the deposition condition.

On the other hand, *M. Kondo* [56] utilized the AFM to study the growth of PEVCD deposited a-Si:H on homo-substrate, in terms of the lattice orientation and surface morphology. At a moderate substrate temperature and under low hydrogen ion bombardment, the surface is significantly roughened. With increasing the temperature or ion bombardment, the lattice orientation is randomized and an amorphous component is increased, resulting in the reduction of the surface roughness. In the substrate dependence studies, substrate orientation and substrate roughness is found affect the surface morphology of the deposited a-Si:H film.

2.7 Hydrogenated Amorphous Silicon

Amorphous silicon when nominally pure is permeated with dangling bonds as evidenced by a detectable electron spin resonance (ESR) signal from about $5x10^{19}$ spins cm^{-3} [7]. The electron energy levels of the dangling bonds lie in between the valence and conduction band states of the fully paired electrons. These states in the energy gap contribute to the optical absorption and electrical conduction process. Further there is a large density of gap state, which act as fast non-radioactive recombination centers, with the result that the photoconductivity or photoluminescence is uninteresting small in pure amorphous silicon. Finally, the fermi level does not have move significantly when trace impurities of conventional shallow donor or acceptor are incorporated. Optimistically, assumed that 'ideal' amorphous silicon can be approached either by annealing procedures [57] or slowly depositing on to substrates at elevated temperature. The annealing will heal the dangling bonds with reconstruction and rearrangement of the amorphous network. However, the annealing effects under certain conditions, are not much reducing the dangling bonds.

If dangling bonds of amorphous silicon can not be paired to each other, the opportunity will exists for other atoms. Hydrogen appears to be most suitable for this purpose. Following the success of the glow discharge plasma decomposition of silane (SiH_4), several other procedures have also evolved for incorporating hydrogen into a-Si. These include reactive sputtering with hydrogen, photon implantation etc. in all case it is presumed that hydrogen passivates the dangling bonds, thereby revealing the interesting properties if intrinsic a-Si [58]. Nuclear reaction and infrared transmission studies shows that incorporation of hydrogen atoms in a-Si matrix reduces 5x1019 to 2x1020 free spin concentration (EPR) of a-Si [59]. Many intrinsic properties of hydrogenated amorphous silicon (a-Si:H) have been studied. These include thermally activated conductivity, optical absorption edge, photoluminescence, electroluminescence and photoconductivity. By doping the a-Si:H to 'n' type or 'p' type respectively. The phenomena of interesting to single crystal silicon become possible to study with a-Si:H. Extrinsic conductivity, thermopower, Hall effect, photoconductivity have all been measure for a-Si:H. Schottky barrier and pn junction diodes have been fabricated with amorphous silicon. When operated as solar cells these diodes behave almost like crystal devices.

In passivated dangling bonds, hydrogen or other additives might passivating the gap states and also play actives roles by enlarging the band gap, changing the electron lattice-coupling and etc. How much hydrogen is needed to reveal the most interesting phenomena is still an open question. In summary, a-Si:H with interesting semiconductor properties has been revealed by the hydrogenation of dangling and weak bonds.

References

1. M.A. Omar, "*Elementally Solid State Physics* ", Addison wesley (1987).
2. S.R. Elliott, "*The Physic and Chemistry of Solids*", Wiley (1998).
3. J.C. Brice , "*Solid State Physics*", ad. E. P. Wohifarth (1973).
4. Iga, Ken 'inchi' 1940, "*Process Technologies for Semiconductor: Crystal Growth & Microprocess*", Berlin Springer (1996).
5. J.D. Joannopoulos, G. Lucovsky, "*The Physics of Amorphous Hydrogenated Silicon I*", (1984).
6. J. Tauc, "*Amorphous and Liquid Semiconductor*", Plenum (1974).
7. M.H. Brodsky, "*Amorphous Semiconductor*", Topic in Applied Physics, Vol. 36, Springer-Verlag (1979).
8. Y. Hamakawa, "*Amorphous Semiconductor Technologies and Devices*", North-Holland (1982).
9. P.A. Walley, "*Thin Solid Films* 2", P237 (1968).
10. B.H. Brodsky, "*Amorphous Semiconductor*", Springer-Verlag 2-3(1985).
11. G. Turbon, Y. Catherlae and B. Grollean, "*Thin Solid Film*", 60-147, (1979).
12. Behaish, R., ed. 1981, "*Sputtering By Particle Bombardment I*", Topics Applied Phys. 47, Springer-Verlag (1981).
13. D.E. Carlson, "*Solar Energy Conversion*", Springer-verlag 12, (1984).
14. R. Behaish , ed. 1983, "*Sputtering By Particle Bombardment II*", Springer-Verlag (1983).
15. R. Behaish, ed. 1991, "*Sputtering By Particle Bombardment III*", Springer-Verlag (1991).
16. R.M. Barrier, "*Hydrothermal Chemistry of Zeolites*". Academic Press: London (1982).
17. M. Hirose, M. Taniguchi, T. Nakashita, Y. Osaka, T. Suzuki, S. H. and T. S., *J. Non-crys. Solid*, 35 & 36 (1980).
18. Yashida, A., Inoue, K., Oshashi, H. and Saito, Y., *Apply Phys. Lett.* , 57, 484, (1979).
19. Masataka Hirose, "*Amorphous Semiconductor Technologies & Devices*", North-Holland, 34, (1985).
20. H.F. Sterling, R.C. G. Swam, *Solid State Elecrochem.* , 8, 653-684 , (1965).
21. H. Meiling, J. Bezemer, R.E.I. Schropp and W.F. Van Der Weg. : *Mat. Res. Soc. Symp. Proc. Vol. 567*, Materials Research Society (1997).

22. J.L. Andujar, E. Bertran, A. Canillas, C. Roch and J.C. Morenze, *J. Vac. Sci. Technol. A9*, 2216, (1991).
23. Richter, H. and Breitling, G., *Z. Naturforsh* , 13a, 988 (1958).
24. Brodsky, M.H., Title, D.S., Weiser, K. and Retit, *G. D. Phys. Rev.* , B1, 2632, (1970).
25. Sec. Ehrenreich, H. and Tumbull, D., "*Comments on Solid States Phys.: For a Brief Discussion of these Model* ", 3, 75 (1970).
26. Light, T. B. and Wagner, C.N.J. , *J. Appl. Cryst.* , 199 (1968).
27. David Adler, "*Amorphous Semiconductor*", Butterworths (London) (1972).
28. Grigovovici, R. and Manaila, R., "*Thin Solid Films*", 1, 343 (1968).
29. Coleman, M.V.A., D. Thomas, D.J.D., *Phys. Status Solids*, 24, k11 (1967).
30. Polk, D.E., *J. Non-Crys. Solid*, 5, 365, (1971).
31. Zachariasen, W.H., J.Amer, *Chem. Soc.* , 54, 3841 (1932).
32. Moss, S.C. and Graczyk, J.F., *Pro. Tenth Int. Conf. Phys. Semi., Cambridge, Mass, 1970, U.S.A.E.C, Div. Tech. Inform.* , *Oak Ridge, Tenn.* , 645 (1970).
33. Cohen, M.H. and Turnball, D., *J. Nature*, 203, 964 (1964).
34. Cohen, M.H., *Pro. Tenth Int. Conf. Phys. Semi., Cambridge, Mass, 1970, U.S.A.E.C, Div. Tech. Inform.* , *Oak Ridge, Tenn.* , 645 (1970).
35. John M. Essick and Richard, T Matter, *Am. J. Phys.* , 61, 11 (1983).
36. Yashihiro Hishikawa, Nobora Nakamura, S. Fsuda, S. Nakano, Y. Kishi and Y.K., *Jpn. J. App. Phys.* , 30, 1008 (1991).
37. R. Swanepoei, *J. Phys. E. : Sci. Instrum. 16*, 11 (1983).
38. J.C. Manifacier, J. Gasiot and J.P. Filand, J. *Phys. E: Sci. Instrum. 9*, 1002 (1978).
39. K.L Chopra, "*Thin Film Phenomena*", McGraw Hill (1969).
40. J. Chaudhuri, S. Shah and J. P. Harbison, *J. Appl. Phys. 66*, 5373 (1989).
41. E.A. Davis, N. Piggins, and S.C. Bayliss, *J. Phys. C: Solid State Phys. 20*, 4415 (1987).
42. D. Bhattacharyga, S.K.B., S. Chaudhuri and A.K. Pal. , *Vacuum 40*, 979 (1993).
43. R.C.Ross and R.Messier, *J. Appl. Phys. (USA), 52(8)*, p. 5329-39, Aug. (1981).
44. R.C.Ross and R.Messier, *J. Appl. Phys. (USA), 56(2)*, p. 5347-51, Aug. (1981).
45. E.C. Freeman and W. Paul, *EMIS Handbook Type Recod RN=4219*, "*Energy Gap of Amorphous Silicon Films Prepared by Various Methods*", (1979).
46. K. Tanaka, S. Yamaski, K. Nakagawa, A. Matsuda, H. Oshuki, M. Matsumura and S. Iizima, *J. Non-Cryst. Solids, 35&36*, P.475-480 (1980).
47. P.W. Anderson, *Phys. Rev. 109*, P.1492 (1958).

48. N.F. Mott, *Philos. Mag. 22*, P.7 (1970).

49. Moustakas, T.D., Anderson, D.A. and W. Paul , *Solid State Commun. 23*, p.115 (1977).

50. J.L. Andujar, E. Bertran, A. Canillas, C. Roch and J.C. Morenze, *J. Vac. Sci. Technol. A9*, 2216 (1991).

51. U.K. Das, P. Chandhuri and S.T. Kshirsagar, *J. Appl. Phys. 80(9)*, p.5389-97, Nov (1996).

52. AFM experiment manual books, *Digital instrument " Nanoscope III "*, (1996).

53. J.C. Knigths and R.A. Rujan, *Appl. Phys. Lett. 35*, 244, (1979).

54. Daewon Kwon and J. David Cohen, *"An AFM Study of The Effect of Growth Method and Conditions on The Microstructure of a-Si:H "*, *Phys. Res.*, (1997).

55. B.G. Budaguan, A.A. Aivazov and M.N. Meytin, *Mat. Res. Soc. Proc. 426, 31* (1996).

56. M. Kondo, Y. Toyoshima, A. Matsuda and K. Ikuta, *J. Appl. Phys.* 80, (1996).

57. Adam Levis, *Phys. Pev. Lett.*, 29 (no.23) 1555, (1972).

58. Hajime Shirai, Jun-inchi Hama and Isma Shimizu, *Jap. J. Appl. Phys.* , 30 (no.4B) L.679, (1991).

59. A. Daneaville, A. Mini and J.C. Brayere, *J. Phys. C. Solid State Phys.*, 14, 4531, (1981).